AFRL-AFOSR-JP-TR-2017-0030

Develop Charge-Selective Interfacial Materials for Polymer & Pervskite SolarCell

Alex K Y Jen
UNIVERSITY OF WASHINGTON

01/25/2016
Final Report

Air Force Research Laboratory
AF Office Of Scientific Research (AFOSR)/ IOA
Arlington, Virginia 22203
Air Force Materiel Command

REPORT DOCUMENTATION PAGE

Form Approved
OMB No. 0704-0188

1. REPORT DATE *(DD-MM-YYYY)*	2. REPORT TYPE	3. DATES COVERED *(From - To)*
10-04-2017	Final	27 May 2014 to 26 Nov 2015

4. TITLE AND SUBTITLE
Develop Efficient Charge-Selective Interfacial Materials for Polymer and Pervskite Solar Cells

5a. CONTRACT NUMBER

5b. GRANT NUMBER
FA2386-14-1-4066

5c. PROGRAM ELEMENT NUMBER
61102F

6. AUTHOR(S)
Alex K Y Jen

5d. PROJECT NUMBER

5e. TASK NUMBER

5f. WORK UNIT NUMBER

7. PERFORMING ORGANIZATION NAME(S) AND ADDRESS(ES)
UNIVERSITY OF WASHINGTON
4333 BROOKLYN AVE NE
SEATTLE, WA 981950001 US

8. PERFORMING ORGANIZATION REPORT NUMBER

9. SPONSORING/MONITORING AGENCY NAME(S) AND ADDRESS(ES)
AOARD
UNIT 45002
APO AP 96338-5002

10. SPONSOR/MONITOR'S ACRONYM(S)
AFRL/AFOSR IOA

11. SPONSOR/MONITOR'S REPORT NUMBER(S)
AFRL-AFOSR-JP-TR-2017-0030

12. DISTRIBUTION/AVAILABILITY STATEMENT
A DISTRIBUTION UNLIMITED: PB Public Release

13. SUPPLEMENTARY NOTES

14. ABSTRACT

This research projects combines highly conductive and robust ETL, HTL and fullerene self-assemble monolayer (SAM) in order to establish a very solid material foundation for enabling the fabrication of multi-junction organic and perovskite solar cells to reach high efficiency, low-cost, and good stability. To gain insights in these material and device development, advanced X-ray and ultrafast spectroscopy are being utilized to probe local carrier dynamics under working conditions such as varied carrier densities and electric fields. By applying these tailored interfacial materials and advanced probing methods to both organic and perovskite active layers, the research team has gained a better understanding of the sought-after connections between molecular structure and performance necessary to reach theoretical efficiency limits. New electron-transporting material (ETM), hole-transporting material (HTM), and self-assemble monolayer (SAMs) are being developed and optimized to meet criteria for organic/perovskite hybrid PVs: i) having the ability to promote Ohmic contact between the electrodes and the active layer; ii) possessing sufficient conductivity and proper energy levels for efficient charge transport and selectivity to reduce resistive loss; iii) having large bandgap to confine excitons in the active layer and low absorption in Vis-NIR to minimize optical loss; iv) possessing proper surface energy to guide the morphology evolution of active layer; (vi) having robustness to support multilayer solution processing. A systematic molecular engineering of these organic/hybrid components is being conducted to tune their electronic/optical properties to enable the fabrication of highly efficient single- and multi-junction organic/hybrid solar cells.

15. SUBJECT TERMS
nanoscience, AOARD

16. SECURITY CLASSIFICATION OF:			17. LIMITATION OF ABSTRACT	18. NUMBER OF PAGES	19a. NAME OF RESPONSIBLE PERSON
a. REPORT	b. ABSTRACT	c. THIS PAGE			CASTER, KENNETH
Unclassified	Unclassified	Unclassified	SAR	12	19b. TELEPHONE NUMBER *(Include area code)* 315-229-3326

Final Report for AOARD (FA2386-14-1-4066**)**

"Developing Efficient Charge-Selective Interfacial Materials for Polymer and Perovskite Solar Cells"

January 20, 2016

Alex K.-Y. Jen, ajen@uw.edu,
University of Washington, Materials Science and Engineering
University of Washington, Seattle, WA 98195-2120

Period of Performance: 5/27/2014 – 11/26/2015

Abstract: As the front-runner photovoltaic materials in solar energy, organometallic halide perovskite have attracted worldwide attention. We have previously identified the interfacial engineering as an important section to optimize the power conversion efficiency of polymer solar cells since it can effectively alleviate the energy barriers existed at the interfaces in the mutli-layered architecture to facilitate the charge transport/extraction in the device. Based on this achievement, the focus of our AOARD project sponsored in this period is to develop efficient charge-transporting interlayers (CTLs) to improve the performance and stability of thin-film perovskite solar cells (PVSCs). We first develop a solution processable, doped transition metal oxide-based hole-transporting interlayer (HTL) to significantly improve the photovoltaic performance and environmental stability of thin-film PVSCs, wherein we elucidate the doping efficacy in the p-type inorganic semiconductors. In addition to the development of HTLs, we also systematically investigate the functions of the commonly used fullerene-based ETLs in conventional p-i-n PVSCs. We not only manifest the conductivity of the employed fullerene-based ETLs has a great impact on the resulting device performance but also reveal the unique electron-coupling between fullerene and perovskite. With the achievement reported in this report, we pave the foundation to continue the optimization in efficiencies with.

Introduction:

Since the seminal discovery by Miyasaka *et al.* in 2009 revealing the potential of perovskite photovoltaics, the tide of organo-metal halide perovskites has surged in the solar cell field.[1] The appealing advantages of perovskites include not only their superior optoelectronic properties, such as intense broad-band absorption, high charge carrier mobility, and long charge diffusion length, but also low-cost precursor materials and simple solution-processable thin-film preparation. These merits have allowed the significant progress of perovskite photovoltaics with power conversion efficiencies (PCEs) rapidly increasing from 3.8 to over 21 % within 6 years.[2]

Typical device configurations of perovskite solar cells (PVSCs) consist of a methylammonium lead halide ($MAPbX_3$, X = Br^-, Cl^-, or I^-) as the photoactive layer and hole-/electron-transporting interlayers sandwiched by collecting electrodes. In general, the positions of the highest occupied molecular orbital (HOMO) (or valence band (VB)) and the lowest unoccupied molecular orbital (LUMO) (or conduction band (CB)) of hole- and electron-transporting layers (HTLs and ETLs), respectively, are of fundamental importance in PVSCs for maximizing charge extraction rates and minimizing energy loss. Among the

PVSC device architectures developed so far, the planar heterojunction configuration attracts particular attention due to its relatively simple device fabrication process. In this regard, the development of facile solution processable CTLs becomes important complements to thin-film PVSCs.

To date, promising power conversion efficiencies (PCEs) have been achieved in such planar geometries based on organic HTLs such as poly(3,4-ethylenedioxythiophene): poly(4-styrenesulfonate) (PEDOT:PSS), poly-triarylamine derivatives, poly-diketopyrrolopyrrole derivatives, and 2,2',7,7'-tetrakis(N,N'-di-p-methoxy-phenylamine)-9,9'-spirobifluorene (spiro-OMeTAD), etc. Compared to organic materials, however, less attention has been paid to the development of inorganic HTLs with favorable energy levels. From the device stability and commercialization points of view, developing alternative inorganic HTLs that can be fabricated through cost efficient means is imperative for the continued evolution of high-performance perovskite photovoltaics. Meanwhile, the most widely used ETLs in the conventional p-i-n structure are mainly based on fullerene derivatives. However, the detailed functions of these fullerene-based ETLs have not been fully exploited yet.

In our original proposal, we first aim to develop the novel charge-selective interfacial materials to enhance the device performance of polymer solar cells (PSCs). With the knowledge and experience regarding interfacial engineering accumulated in PSCs,[3] we continue to develop efficient HTL and ETL for achieving high-performance PVSCs in this extended research period. In first section, we describe a doped NiO_X HTL to realize a high PCE (> 15 %) PVSC showing decent environmental stability. Through the doping strategy, we effectively improve the conductivity of NiO_X without changing its energy levels too much. As a result, the resultant photovoltaic parameters are largely enhanced. Besides, owning to the deep-lying HOMO of NiO_X, we also demonstrate it is very suitable for the high bandgap perovskite with a deeper-lying HOMO than the pristine $CH_3NH_3PbI_3$ ($MAPI_3$). In the second section, we systematically investigate the functions of the commonly used fullerene-based ETLs in conventional p-i-n PVSCs. We manifest the conductivity of the employed fullerene-based ETLs has a great impact on the resulting device performance. Moreover, we further reveal the unique electron-coupling between fullerene and perovskite.

Results and Discussion:

(1) Development of a solution-processed copper-doped nickel oxide hole-transporting layer for efficient and environmentally stable planar heterojunction perovskite solar cells

Among the developed inorganic p-type HTL for PVSCs, nickel oxide (NiO_x) has attracted the most interests nowadays due to its large band-gap (E_g) for well electron-bloc king capability.[4-8] Moreover, NiO_x possesses other advantages like energetically favorable energy level alignment with photoactive layers with a deep-lying HOMO (or VB) as well as good environmental stability. However, the photovoltaic performance of NiO_x in PVSCs, in particular solution-processed NiO_x, is still not satisfactory when compared to devices based on PEDOT:PSS and other organic HTLs because of lower fill factor (FF) or short circuit current densities (J_{SC}) in spite of the significantly improved V_{OC}.[8-11] Doping can mitigate such losses in FF and J_{SC} through its capacity to modulate conductivity, as is evidenced by the engineering behind the HTLs used currently in PVSCs.[12-15] Providing the superior chemical stability and compositional variety of inorganic HTLs, we are interested in exploring the doping efficacy in NiO_X HTL to further optimize the photovoltaic performance

of the derived PVSCs. In this work, we have demonstrate high-efficiency planar heterojunction PVSCs based on solution-processed copper (Cu)-doped NiOx ($Cu:NiO_x$) showing an impressive PCE up to 15.40 % with decent environmental stability (**Figure 1**). Note that Cu is employed as a dopant here due to its unique electronic and structural effects as well as the ease to be incorporated into the solution fabrication of NiO_x.[16-17] Besides, the studied PVSC is based on a conventional configuration of indium tin oxide (ITO)/HTL (PEDOT:PSS, pristine NiO_x or $Cu:NiO_x$)/perovskite/$PC_{61}BM$/C_{60}-bis surfactant/silver (Ag).

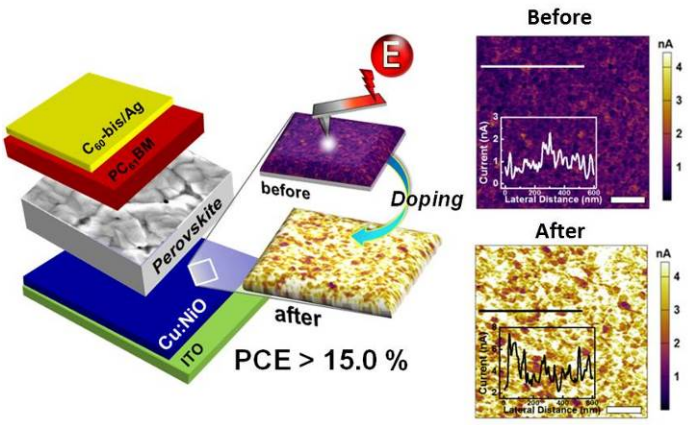

Figure 1. Scheme of the studied device configuration and the c-AFM images of pristine NiO_x (purple) and $Cu:NiO_x$ films (brown) at V_{bias} = 1.0 V. Scale bar: 200nm; Inserts: current profiles obtained from the solid line in the images.

We first characterize the influence of Cu-doping on the electrical conductivity of NiO_X, and compare the conductivity of pristine NiO_X and $Cu:NiO_X$ films by performing conductive atomic force microscopy (c-AFM), as revealed at the right-hand side of **Figure 1**, which clearly show different current level and distribution between them. Significantly increased vertical current is observed in the $Cu:NiO_X$ film, suggesting increased electrical conductivity upon Cu-doping. Notably Chen *et al.* observed an increase in carrier concentration with increasing Cu content (~9-18 at.%) that is accompanied by a sharp mobility decrease. Additionally, increasing Cu content monotonically reduces the transmittance of the material. **[15]** These optoelectronic impacts are accompanied by the generation of large NiO_x grain, a tendency which may be linked to the unique defect chemistry involved. These considerations illustrate that while clearly valuable, there is likely a diminishing return with respect to Cu doping.

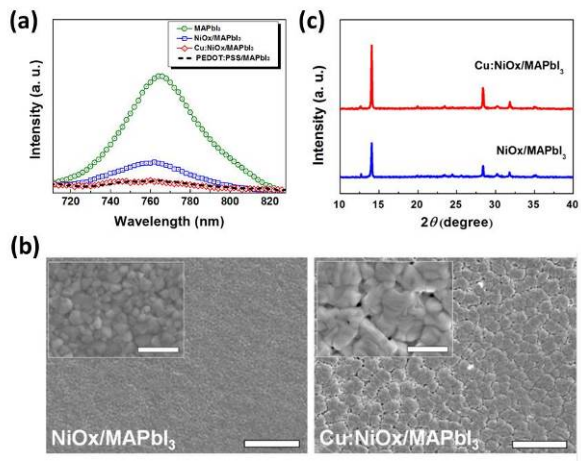

Figure 2. (a) PL spectra (excitation at 600 nm) of $MAPbI_3$ films on top of pristine NiO_x (squares), $Cu:NiO_x$ (diamonds) and PEDOT:PSS (dotted line). (b) SEM images and (c) XRD of $MAPbI_3$ films on top of pristine NiO_x and $Cu:NiO_x$. (Scale bars are 5 μm and 1 μm (inset)).

Since the pristine NiO_X and $Cu:NiO_X$ are employed as HTLs in PVSCs, photoluminescence (PL) measurement was conducted to investigate their quenching efficiency for the photo-generated carriers in the perovskite absorber. As shown in **Figure 2a**, the $MAPbI_3$ film shows considerably greater PL quenching on Cu:NiOx than pristine NiOx, indicating its enhanced efficiency in hole collection and transport, which follows naturally from the increased electrical conductivity. Note that the $Cu:NiO_x$ film exhibits comparable PL quenching to PEDOT:PSS, demonstrating its viability in replacing PEDOT:PSS for high-performance

PVSCs.

Film formation and surface morphology of the perovskite absorber has proven to be crucial for the resultant device performance. Hence, the scanning electron microscopy (SEM) measurements were performed to understand the perovskite crystallization on the studied NiO_X HTLs, as presented in **Figure 2b**. Interestingly, despite slightly reduced coverage, the perovskite film grown on Cu:NiO_X shows larger grain size (~1 μm) compared to the film on pristine NiO_X (~300 nm), which might originate from the different surface morphologies of pristine and Cu-doped NiO_X films as grain size increases upon Cu-doping. NiO_X surface chemistry may also be dependent on Cu content, which is a possible factor influencing nucleation behavior and promoting the sustained growth of more widely dispersed nuclei. Perovskite film quality was further analyzed by X-ray diffraction (XRD). As displayed in **Figure 2c**, intense XRD signal is observed for the crystalline $MAPbI_3$ films grown on both of them.

The photovoltaic performance of the studied devices derived from pristine NiO_X and Cu:NiO_X HTLs under AM 1.5 G conditions (100 mW cm^{-2}) are shown in **Figure 3a** and **Table 1**. As expected, the pristine NiO_X-based solar cell exhibit higher V_{OC} (1.08 V) than the PEDOT:PSS-based device (0.91 V). As previously reported, this can be ascribed to the reduced potential loss at the HTL/perovskite interface due to the improved energy level alignment. However, the relatively low J_{SC} (14.03 mA/cm^2) and FF (0.59) of the pristine NiO_X-based solar cell led to a lower PCE (8.94%) than that of the PEDOT:PSS-based device (11.16%). Employing the Cu:NiO_X as the HTL has significantly improved device performance, particularly J_{SC} and FF, due to its improved electrical conductivity relative to NiO_X. It results in a PCE_{MAX} of 15.40% with V_{OC}, J_{SC} and FF of 1.11 V, 19.01 mA/cm^2 and 0.73, respectively, which substantially surpass the performance of PEDOT:PSS-based device. Moreover, the series resistance (R_s) of the NiO_x-based solar cell reduced from 9.49 to 6.89 cm^{-2} upon doping. This improvement in device performance by using doped NiO_x is similar to the trend in perovskite solar cells employing doped organic HTLs.

External quantum efficiency (EQE) spectra of the studied devices are shown in **Figure 3b**. The PVSC based on Cu:NiO_x possesses much higher photon-to-electron conversion as compared to the pristine NiO_x-based device, confirming that the simple Cu-doping of NiO_x is an effective way to improve device performance by increasing its electrical conductivity, charge extraction efficiency, and favorable perovskite crystallization. In addition, the hysteresis of a Cu:NiO_X-based solar cell was examined by varying scan rate and the device exhibited negligible hysteresis at a high scan rate (1.0 V s^{-1}) and slight hysteresis gradually appeared as the scan rate decreased (towards 0.05 V s^{-1}), which might arise from interfacial traps induced in solution-processed NiO_X.

PEDOT:PSS has been widely used as a HTL for high-performance planar heterojunction

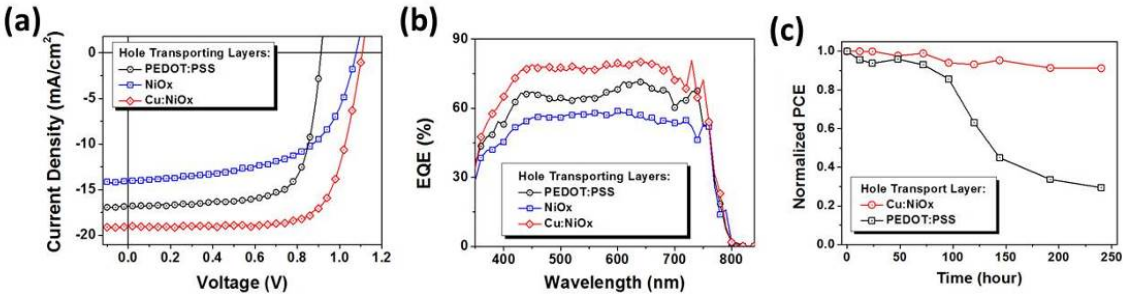

Figure 3. (a) *J–V* curves and (b) EQE spectra of PVSCs based on PEDOT:PSS (circles), NiO_x (squares) and Cu:NiO_x (diamonds) HTLs. (c) Normalized PCE of the studied PVSCs based on PEDOT:PSS (squares) and Cu:NiO_x (circles) HTLs as a function of storage time in air.

Table 1. Summarized solar cell parameters based on different hole transporting layers (HTLs).

HTL	V_{OC} [V]	FF	J_{SC} [mA cm^{-2}]	PCE [%]
PEDOT:PSS	0.90 ± 0.01	0.73 ± 0.01	16.64 ± 0.55	10.87 ± 0.29 (11.16)
NiO_x	1.08 ± 0.01	0.58 ± 0.01	14.13 ± 0.29	8.73 ± 0.13 (8.94)
5 at.% Cu:NiO_x	1.11 ± 0.01	0.72 ± 0.01	18.75 ± 0.42	14.98 ± 0.33 (15.40)

Average values with standard deviation (maximum values are in parentheses)

PVSCs; however, its acidic and hygroscopic properties and inability to block electrons efficiently are problematic for device stability. To verify this, the air-stability of $MAPbI_3$ PVSCs without encapsulation was characterized and is presented in **Figure 3c**. The Cu:NiO_X -based solar cell shows markedly improved air-stability as compared to the PEDOT:PSS-based device. The PCE of the Cu:NiO_X-based device remains above 90 % of the initial value even after 240 h of storage in air. In contrast, the PEDOT:PSS-based device degraded to < 50% of its initial PCE within 144 h of storage in air, which was mainly caused by the gradual decrease in FF and J_{SC}. As aforementioned, this lower stability might originate from the acidic and hygroscopic characteristics of PEDOT:PSS that degrade the ITO electrode and the adjacent moisture-sensitive photoactive (perovskite) layer.

We further extend the applicability of a Cu:NiO_X layer to large E_g perovskite systems, $MAPb(I_XBr_{1-X})_3$ which have deeper-lying VB than $MAPbI_3$, for improving their performance because of better matched energy level between the VB of Cu:NiO_x and perovskite. It is well documented that the increased E_g of such Br-based perovskites accompany the simultaneous upshift of LUMO and downshift of HOMO relative to the pristine $MAPbI_3$. In this regard, the deep VB of NiO_x can provide better energy alignment with large E_g Br-based perovskites (VB below 5.4 eV) than PEDOT:PSS (5.2 eV). Devices based on large E_g perovskites ($MAPb(I_{0.8}Br_{0.2})_3$ and $MAPb(I_{0.6}Br_{0.4})_3$) were fabricated with the same device configuration as mentioned above. As shown in **Figure 4**, the Cu:NiO_x-based large E_g solar cells indeed show much higher V_{OC} than the PEDOT:PSS-based large E_g devices (**Figure 4b**), which confirms superior energy level alignment with large E_g perovskites. In addition to the improved V_{OC}, the FF of the Cu:NiO_X -based large E_g solar cells also exceeds those of the PEDOT:PSS-based large E_g devices (**Figure 4c**), which originates from the high electrical conductivity of Cu:NiO_X. As shown in **Figure 4d**, the Cu:NiO_X -based solar cells preserve higher V_{OC}/E_g values of 0.65 ($MAPb(I_{0.6}Br_{0.4})_3$), 0.68 ($MAPb(I_{0.8}Br_{0.2})_3$) and 0.71 ($MAPbI_3$) than the PEDOT:PSS-based devices (0.56, 0.58 and 0.59), suggesting that the latter system suffers relatively large potential losses (E_g–V_{OC}: 0.78, 0.70 and 0.64 for PEDOT:PSS-based devices; 0.62, 0.52 and 0.45 for Cu:NiO_X -based devices). These results clearly reveal the efficacy of a Cu:NiO_X HTL in conjunction with

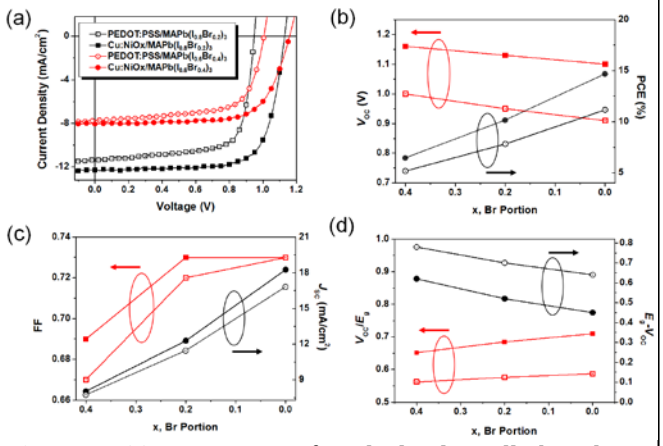

Figure 4. (a) *J–V* curves of studied solar cells based on PEDOT:PSS (opened squares and opened circles) and Cu:NiO_x (filled squares and filled circles) for $MAPb(I_{0.8}Br_{0.2})_3$ and $MAPb(I_{0.6}Br_{0.4})_3$, respectively. Variation of V_{OC} and PCE (b), FF and J_{SC} (c), and E_g-V_{OC} and V_{OC}/E_g of studied solar cells based on PEDOT:PSS (opened squares and opened circles) and Cu:NiO_x (filled squares and filled circles) , where x=0, 0.2, 0.4.

large E_g Br-based perovskites, which effectively reduces the potential losses and enhances PCE due to its deeper VB.

This work not only reveals the importance of doping in designing more effective inorgan ic transporting interlayers, but also provides an excellent device platform for making high-p erformance multi-stacked perovskite tandem solar cells.

(2) Exploring the roles of fullerene-based interlayers in enhancing the performance of organometal perovskite thin-film solar cells

In the previous section, we have developed an efficient Cu:NiOx HTL for fabricating a high-performance conventional PHJ PVSC (configuration: substrate/HTL (p)/perovskite (i)/fullerene derivative (n)). As mentioned previously, thin-film planar heterojunction (PHJ) PVSCs have been actively pursued due to their relatively simple device fabrication process. Therefore, besides developing new HTLs for highly efficient PVSCs, we simultaneously investigate the roles of the commonly used fullerene-based electron-transporting layer (ETLs) in such conventional device configuration.[8,12,19] It is worth noting that room temperature, orthogonal solvent processability of fullerene derivatives can successfully prevent the degradation of the underlying perovskite layer. Moreover, their decent electron mobility makes them as promising ETLs for high-performance PVSCs. In addition to $PC_{61}BM$, various fullerene derivatives have also been utilized as efficient ETLs in PVSCs.[19-20] All these independent results highlight the importance of fullerene-based ETLs in enhancing device performance. However, large discrepancies documented in the literature for each system suggest that a systematic study to investigate the influence of the charge-transporting properties of fullerene ETLs on device performance is warranted. Besides, the interaction between perovskite and fullerene remains unclear at present. For this reason, it is important to understand the roles of these fullerene-based ETLs in PVSCs, especially in terms of their intrinsic properties and interaction at the perovskite/fullerene interface.

In this work, we demonstrate a clear correlation between the charge-transporting properties of fullerene-based ETLs and photovoltaic performance by systematically studying three fullerenes, ICBA, PCBM, and C (**Figure 5**). We first verified the electron mobility of the studied fullerenes by field-effect transistors (FETs). As shown in **Figure 6a**, the electron mobility gradually increases from $IC_{60}BA$ (6.9 x 10^{-3} cm^2/Vs), to $PC_{61}BM$ (6.1 x 10^{-2} cm^2/Vs), to C_{60} (1.6 cm^2/Vs) due to the increased conjugation of fullerene core. Note that C_{60}'s lack of bulky side-chains allows it to be packed more densely, which facilitates intermolecular charge transport and further enhances electron mobility

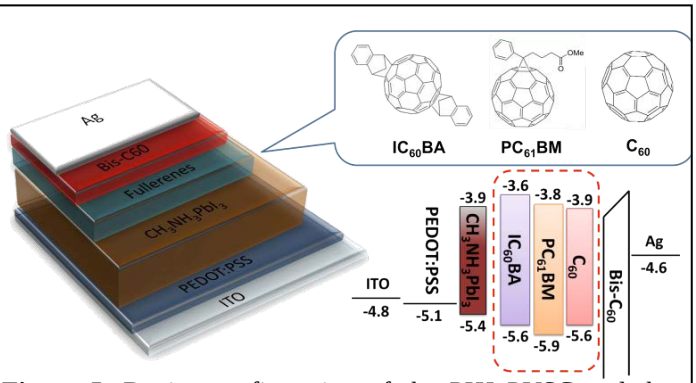

Figure 5. Device configuration of the PHJ PVSC and the chemical structures of the n-type fullerene derivatives, $IC_{60}BA$, $PC_{61}BM$ and C_{60} in this study. The energy diagram of the each layer in devices.

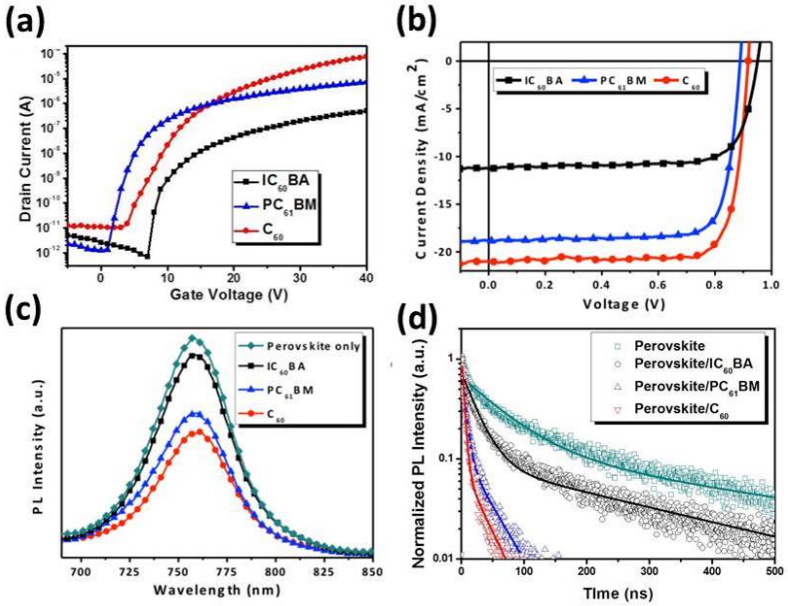

Figure 6. (a) The FET transfer characteristics of the studied fullerenes. (b) *J-V* curves of the studied PVSCs using different fullerene-based ETLs. (c) Steady-state PL spectra of perovskite in the presence of the studied fullerene quenchers. (d) Time-resolved photoluminescence characterization of the solution-processed pervoskite without and with three fullerene derivatives.

To elucidate the influence of electron mobility of fullerene-based ETLs on the photovoltaic performance of PVSCs, a conventional device configuration of ITO/PEDOT:PSS (35-40 nm)/$MAPbI_3$ (300 nm)/fullerenes (~60 nm)/Bis-C_{60} (10 nm)/Ag (150 nm) was fabricated. All the fullerene ETLs are spin-cast for fair comparison. The deposition of the $MAPbI_3$ thin film followed the solvent-washing method reported by Seok *et al.*[21] which provides a smooth perovskite thin film with good surface coverage on PEDOT:PSS. We also revealed that crystallinity of perovskite are almost unaffected by the deposition of fullerene layers. The *J-V* curves of the studied devices are shown in **Figure 6b** and the relevant photovoltaic performance are summarized in **Table 2**. Impressively, the C_{60}-based device afforded the highest PCE_{MAX} of 15.44% with a V_{OC} of 0.92 V, a J_{SC} of 21.07 mA/cm^2, and a FF of 0.80. The $PC_{61}BM$- and $IC_{60}BA$-based devices showed PCEs of 13.37% (V_{OC}: 0.89 V, J_{SC}: 18.85 mA/cm^2, and FF: 0.80) and 8.06% (V_{OC}: 0.95 V, J_{SC}: 11.27 mA/cm^2, and FF: 0.75), respectively.

Interestingly, the $IC_{60}BA$-derived device showed the highest V_{OC} which can be rationalized from the fact that its LUMO is the highest among the three fullerenes. This high-lying LUMO is beneficial in maintaining the high-lying electron quasi-Fermi levels ($E_{F,e}$) in the perovskite-based p-i-n heterojunction under illumination. This results in a relatively large built-in voltage across the device while the quasi-Fermi levels of holes ($E_{F,h}$) in the p-i-n heterojunction are kept fixed by the PEDOT:PSS/perovskite interface.

Table 2. The photovoltaic performance of the studied PVSCs using different fullerene-based ETLs.

Employed Fullerene	V_{OC} (V)	J_{SC} (mA/cm^2)	FF	PCE (%)	R_s (Ω cm^2)	R_{sh} (kΩ cm^2)
$IC_{60}BA$	0.95	11.27	0.75	8.06	5.10	0.71
$PC_{61}BM$	0.89	18.85	0.80	13.37	2.60	3.14
C_{60}	0.92	21.07	0.80	15.44	2.26	8.72

Average values with standard deviation (maximum values are in parentheses)

Consequently, the C_{60}-based PVSC should have the smallest V_{OC} of the three fullerenes because of C_{60}'s low LUMO. However, the C_{60}-based PVSC showed a comparable V_{OC} (0.92 V) to that of $PC_{61}BM$-based device (0.89 V). It can be envisaged that high C_{60} electron mobility effectively reduces charge recombination at the perovskite/C_{60} interface and diminishes potential loss across this interface. Besides, the hysteresis test of the studied devices was also performed. All the devices presented very minor hysteresis at a low scan rate of 0.01 V/s, suggesting limited charge traps at the perovskite interfaces (PEDOT:PSS/$MAPbI_3$ and $MAPbI_3$/fullerene).

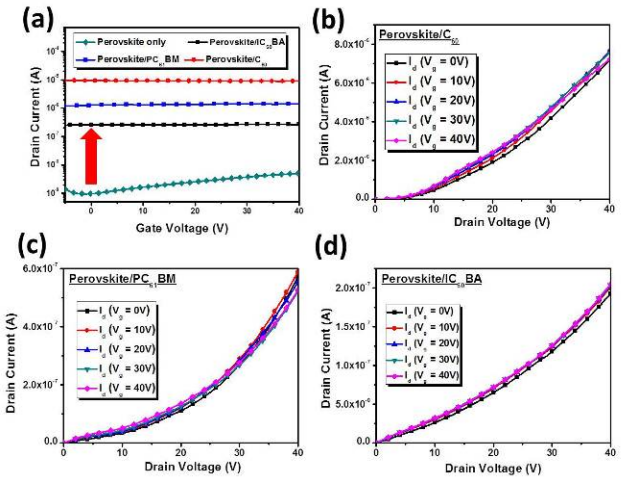

Figure 7. The FET (a) transfer characteristics of bilayer perovskite/fullerenes devices and the output characteristics of (b) perovskite/C_{60}, (c) perovskite/$PC_{61}BM$, and (d) perovskite/$IC_{60}BA$ FET devices.

The improved J_{SC} and FF of $PC_{61}BM$- and C_{60}-based PVSCs can be interpreted as a consequence of improved charge dissociation/transport at the perovskite/fullerene interface arising from these fullerenes' increased electron mobility, as is evident in the steady-state photoluminescence (PL) spectra (**Figure 6c**). Quenching efficiency of perovskite luminescence follows the trend C_{60} > $PC_{61}BM$ >> $IC_{60}BA$, which is consistent with the trend of electron mobility. To obtain more in-depth information, the lifetime of perovskite without and with three fullerene derivatives are evaluated by the time-resolved photoluminescence (TR-PL) and the results are shown in **Figure 6d**. Considering the perovskite/fullerene case, fullerene quenchers mainly contributed to the fast quenching processes. Both analyses demonstrated that C_{60} is the most efficient quencher among all three fullerene derivatives, suggesting that free charges carriers can dissociate efficiently at the perovskite/C_{60} interface rather than recombined inside the perovskite layer. All these results affirm that the high electron mobility of fullerene ETLs can enhance the photovoltaic performance of PVSC. More importantly, C_{60} is also more cost-effective than PC61BM. Given its comparable room-temperature solution processability, it is economically superior as well.

In addition to elucidating the influence of fullerene derivative's mobility, we have also examined the electrical characteristics of bilayer perovskite/fullerene field-effect transistors (FETs). Interestingly, metallic conduction in the bilayer perovskite/fullerene film was observed as depicted in **Figure 7a**, signifying that effective interfacial interaction exists under bias between perovskite and fullerene. Taking C_{60} for example, the perovskite/C_{60} FET shows a six order higher current than the pristine C_{60} FET at V_G = 0 V (**Figure 6a&7a**) while the $IC_{60}BA$- and $PC_{61}BM$-based devices also exhibit similar phenomena but with lower degrees of enhancement. The estimated intrinsic conductivities (at V_G = 0 V) for the bilayer $MAPbI_3$/fullerene devices are 2.4 × 10^{-3} S/cm (for $MAPbI_3/C_{60}$), 3.2 × 10^{-4} S/cm ($MAPbI_3/PC_{61}BM$), and 6.5 × 10^{-5} S/cm ($MAPbI_3/IC_{60}BA$), respectively. These results suggest that charge transfer occurs spontaneously between perovskite and fullerenes, and that the degree of charge transfer is correlated with mobility and fullerene molecular structure. The very minor hysteresis and high performance of PVSCs studied herein show

that such charge redistribution at the perovskite/fullerene interface may also passivate interfacial trap states as well as reduce interfacial energy barrier.

The recent finding reported by Huang *et al.*[20,22] echoes this hypothesis to a certain extent as they find that fullerene-based ETLs ($PC_{61}BM$, C_{60}, or $PC_{61}BM/C_{60}$) do passivate the trap density of states at the perovskite surface. Second, charge redistribution can increase the carrier concentration in the fullerene layer, which effectively becomes n-doped by the electrons transferred from the perovskite. Upon doping, the Fermi level of the fullerene film would up-shift to conducting states, thereby reducing contact resistance, enhancing charge extraction, and increasing built-in potential across the device. It can be envisioned that both these phenomena occurring at the perovskite/fullerene interface can effectively reduce the interfacial energy barrier for charge extraction, and thus they are believed to be the dominant factors leading to the very minor hysteresis and high performance of fullerene-based PVSCs.

List of Publications and Significant Collaborations that resulted from your AOARD supported project:

a) Papers published in peer-reviewed journals

1. J. W. Jung, C. C. Chueh, Alex K. Y. Jen, "Low Temperature Solution-Processable Cu-doped Nickel Oxide Hole-Transporting Layer via Combustion Method for High Performance Thin-Film Perovskite Solar Cells" *Adv. Mater.* **2015**, 27, 7874-7880.
2. J. H. Kim, C. C. Chueh, S. T. Williams, Alex K. Y. Jen*, Solution-Processable Organic Electron Extraction Layer for High-Performance Planar "Room-Temperature, Heterojunction Perovskite Solar Cells", *Nanoscale*, **2015**, 7, 17343-17349.
3. J. W. Jung, C. C. Chueh, Alex K. Y. Jen, "High-Performance Semi-Transparent Perovskite Solar Cells with 10% Power Conversion Efficiency and 25% Average Visible Transmittance Based on Transparent CuSCN as the Hole-Transporting Material" *Adv. Energy Mater.* **2015**, 5, 1500486.
4. Z. B. Yang, C. C. Chueh, F. Zuo, J. H. Kim, P. W. Liang, Alex K. Y. Jen, "High-Performance Fully Printable Perovskite Solar Cells via Blade-Coating Technique Under Ambient Condition" *Adv. Energy Mater.* **2015**, 5, 1500328
5. P. W. Liang, C. C. Chueh, S. T. Williams, Alex K. Y. Jen, "Roles of Fullerene-based Interlayers in Enhancing the Performance of Organometal Perovskite Thin-Film Solar Cells", *Adv. Energy Mater.* **2015**, 5, 1402321
6. C. C. Chueh, C. Z. Li, A. K.-Y. Jen, "Recent Progress and Perspective in Solution-Processed Interfacial Materials for Efficient and Stable Polymer and Organometal Perovskite Solar Cells", *Energy & Environmental Science* **2015**, 8, 1160-1189.

b) Conference presentations

1. Invited Talk, "Integrated Molecular Design, Interface Engineering, and Device Processing for Highly Efficient Polymer & Perovskite Solar Cells", International Conference of Science and Technology of Synthetic Metals, Turku, Finland, June-30-July 4, 2014.

2. Colloquium, “Integrated Molecular Design, Self-Assembly, Interface Engineering, and Device Processing for Organic Photonics and Electronics”, Department of Polymer Science & Engineering, Zhejiang University, Hangzhou, China, July 8, 2014.
3. Invited Talk, “Integrated Molecular Design, Interface Engineering, and Device Processing for Highly Efficient Polymer & Perovskite Solar Cells”, Chinese Chemical Society Meeting on OPV, Beijing University, China, August 4-8, 2014.
4. Colloquium, “Molecular Engineering for Creating Societal Impact”, Korean University, Seijong, Korea, August 27, 2014.
5. Colloquium, “Integrated Molecular Design, Interface Engineering, and Device Processing for Highly Efficient Polymer Solar Cells”, Korean University, Seijong, Korea, August 29, 2014.
6. Plenary Talk, “Integrated Molecular Design, Self-Assembly, Interface Engineering, and Device Processing for Polymer Solar Cells”, Polymer Solar Cell Conference, National Chiao-Tung University, Taiwan, September 1-3, 2014.
7. Invited Talk, “Integrated Molecular Design, Interface Engineering, and Device Processing for Highly Efficient Polymer & Perovskite Solar Cells”, Solution Processed Semiconductor Solar Cells Conference, Oxford University, UK, September 9-12, 2014.
8. Invited Talk, “Multi-Functional Self-Assembled Monolayers for Electronic Applications”, Air Force Office of Scientific Research, Joint Review, Arlington, VA, October 28-29, 2014.
9. Invited Talk, “Integrated Molecular Design, Interface Engineering, and Device Processing for Highly Efficient Polymer & Perovskite Solar Cells”, Solar Future 2014, King Abdullah University of Science and Technology, Saudi Arabia, November 8-November 11, 2014.
10. Colloquium, “Molecular Engineering to Create Societal Impact”, Department of Chemistry, Texas A&M University, College Station, Texas, November 14, 2013.
11. Plenary Talk, “Integrated Molecular Design, Interface Engineering, and Device Processing for Highly Efficient Polymer & Perovskite Solar Cells”, Chinese Chemical Society Meeting, Hsin-Chu, Taiwan, November 21-November 24, 2014.
12. Colloquium, “Integrated Molecular Design, Interface Engineering, and Device Processing for Polymer and Perovskite Solar Cells”, Department of Molecular Engineering & Chemistry, Wuhan University, Wuhan, China, December 22, 2014.
13. Colloquium, “Integrated Molecular Design, Interface Engineering, and Device Processing for Polymer and Perovskite Solar Cells”, National Key Laboratory for Optoelectronics, South China University of Technology, Guangzhou, China, December 23, 2014.
14. Colloquium, “Integrated Molecular Design, Interface Engineering, and Device Processing for Polymer and Perovskite Solar Cells”, Department of Materials Science & Engineering, South University of Science & Technology, Shenzhen, China, December 26, 2014.
15. Colloquium, “Integrated Molecular Design, Interface Engineering, and Device Processing for Polymer and Perovskite Solar Cells”, Department of Chemistry, Hong Kong University of Science & Technology, Hong Kong, December 29, 2014.
16. Invited Talk, “Integrated Molecular Design, Interface Engineering, and Device Processing for Polymer ands Pervoskite Solar Cells”, Symposium on “ENERGY & MATERIALS II”, American Chemical Society Meeting, Denver, CO, March 22-24, 2015.

17. Invited Talk, “From Molecular Photovoltaics to Printable Solar Cells”, Paul Weiss Award Symposium, Colloidal Chemistry Division, American Chemical Society Meeting, Denver, CO, March 22-24, 2015.
18. Invited Talk, “Integrated Molecular Design, Interface Engineering, and Device Processing for Highly Efficient Polymer Solar Cells”, Material Research Meeting, San Francisco, CA, April 6-8, 2015.
19. Invited Talk, “Integrated Interface Engineering and Device Processing for Highly Efficient Perovskite Solar Cells”, ANSER Center Annual Symposium, Northwestern University, April 16-17, 2015.
20. Plenary Talk, “From Molecular Photovoltaics to Printable Solar Cells”, 13th International Conference of Polymers for Advanced Technologies (PAT), Hangzhou, China, June 25-28.
21. Invited Talk, “Integrated Molecular Design, Interface Engineering, and Device Processing for Highly Efficient Polymer Solar Cells”, Korean OPV-Photo Science Meeting, Seoul, Korea, August 23-25.
22. Colloquium, “Integrated Molecular Design, Interface Engineering, and Device Processing for Polymer and Perovskite Solar Cells”, Department of Material Chemistry, Korea University, Seijong, Korea, August 26-27, 2015.
23. Invited Talk, “Integrated Molecular Design, Interface Engineering, and Device Processing for Highly Efficient Polymer Solar Cells”, Chinese Polymer Society Annual Meeting, Suzhou, China, October 17-20, 2015.
24. Invited Talk, “Integrated Molecular Design, Interface Engineering, and Device Processing for Polymer ands Pervoskite Solar Cells”, KAIST Renewable Energy Symposium, Denver, Daejeon, Korea, October 29-30, 2015.
25. Colloquium, “From Molecular Photovoltaics to Printable Solar Cells”, Department of Chemistry, National Tsing Hua University, Hsin-Chu, Taiwan, November 23, 2015.
26. Colloquium, “Integrated Molecular Design, Interface Engineering, and Device Processing for Polymer and Perovskite Solar Cells”, Department of Materials Science & Engineering, National Tsing Hua University, Hsin-Chu, Taiwan, November 24, 2015.
27. Invited Talk, “Integrated Molecular Design, Interface Engineering, and Device Processing for Polymer ands Pervoskite Solar Cells”, Pacific Polymer Congress, “Photoconductive, OLEDs, Solar, etc. Symposium, Kauai, Hawaii, December 9-14, 2015.
28. Colloquium, “Integrated Molecular Design, Interface Engineering, and Device Processing for Polymer and Perovskite Solar Cells”, Department of Molecular Engineering & Chemistry, Wuhan University, Wuhan, China, December 25, 2015.
29. Wuhan Optoelectronics Forum, “Integrated Molecular Design, Interface Engineering, and Device Processing for Perovskite Solar Cells”, National Optoelectronics Center, Huazhong University of Science & Technology, Wuhan, China, December 23, 2015.
30. Colloquium, “Integrated Molecular Design, Interface Engineering, and Device Processing for Polymer and Perovskite Solar Cells”, National Key Laboratory for Optoelectronics, South China University of Technology, Guangzhou, China, December 29, 2015.
31. Colloquium, “Integrated Molecular Design, Interface Engineering, and Device Processing for Polymer and Perovskite Solar Cells”, Department of Materials Science & Engineering, South University of Science & Technology, Shenzhen, China, December 30, 2015.

Reference

1. A. Kojima, K. Teshima, Y. Shirai, T. Miyasaka, *J. Am. Chem. Soc.* **2009**, 131, 6050.
2. http://www.nrel.gov/ncpv/images/efficiency_chart.jpg (January, 2016)
3. C. C. Chueh, C. Z. Li, A. K.-Y. Jen, *Energy Environ. Sci.* **2015**, 8, 1160-1189.
4. K.-C. Wang, J.-Y. Jeng, P.-S. Shen, Y.-C. Chang, E. W.-G. Diau, C.-H. Tsai, T.-Y. Chao, H.-C. Hsu, P.-Y.Lin, P. Chen, T.-F. Guo, T.-C. Wen, *Sci. Rep.* **2014**, 4, 4756.
5. M. D. Irwin, B. Buchholz, A. W. Hains, R. P. H. Chang, T. J. Marks, *Proc. Natl. Acad. Sci. U.S.A.* **2008**, 105, 2783.
6. J. R. Manders, S.-W. Tsang, M. J. Hartel, T.-H. Lai, S. Chen, C. M. Amb, J. R. Reynolds, F. So, *Adv. Funct. Mater.* **2013**, 23, 2993.
7. S. Liu, R. Liu, Y. Chen, S. Ho, J. H. Kim, F. So, *Chem. Mater.* **2014**, 26, 4528.
8. J. Y. Jeng, Y. F. Chiang, M. H. Lee, S. R. Peng, T. F. Guo, P. Chen, T.-C. Wen, *Adv. Mater.* **2013**, 25, 3727.
9. Z. Zhu, Y. Bai, T. Zhang, Z. Liu, X. Long, Z. Wei, Z.Wang, L. Zhang, J. Wang, F. Yan, S. Yang, *Angew. Chem. Int. Ed.* **2014**, 53, 1.
10. L. Hu, J. Peng, W. Wang, Z. Xia, J. Yuan, J. Lu, X. Huang, W. Ma, H. Song, W. Chen, Y.-B. Cheng, J. Tang, *ACS Photonics* **2014**, 1, 547.
11. K.-C. Wang, P.-S. Shen, M.-H. Li, S. Chen, M.-W. Lin, P. Chen, T.-F. Guo, *ACS Appl. Mater. Interfaces* **2014**, 6, 11851.
12. J. You, Z. Hong, Y. Yang, Q. Chen, M. Cai, T.-B. Song, C.-C. Chen, S. Lu, Y. Liu, H. Zhou, Y. Yang, *ACS Nano* **2014**, 8, 1674.
13. Y. S. Kwon, J. Lim, H.-J. Yun, Y.-H. Kim, T. Park, *Energy Environ. Sci.* **2014**, 7, 1454.
14. N. J. Jeon, J. Lee, J. H. Noh, M. K. Nazeeruddin, M, Grätzel, S. I. Seok, *J. Am. Chem. Soc.* **2013**, 135, 19087.
15. B. Xu, E. Sheibani, P. Liu, J. Zhang, H. Tian, N. Vlachopoulos, G. Boschloo, L. Kloo, A. Hagfeldt, L. Sun, *Adv. Mater.* **2014,** 26, 6629.
16. K. H. Kim, C. Takahashi, Y. Abe, M. Kawamura, *Optik* **2014**, 125, 2899.
17. M. Yang, Z. Shi, J. Feng, H. Pu, G. Li, J. Zhou, Q. Zhang, *Thin Solid Films* **2011**, 519, 3021.
18. S. C. Chen, T. Y. Kuo, Y. C. Lin, H. C. Lin, *Thin Solid Films* **2011**, 519, 4944.
19. C.-H. Chiang, Z.-L. Tseng, C.-G. Wu, *J. Mater. Chem. A* **2014**, 2, 15897.
20. Z. Xiao, C. Bi, Y. Shao, Q. Dong, Q. Wang, Y. Yuan, C. Wang, Y. Gao, J. Huang, *Energy Environ. Sci.* **2014**, 7, 2619.
21. N. J. Jeon, J. H. Noh, Y. C. Kim, W. S. Yang, S. Ryu, S. I. Seok, *Nature Mater.* **2014**, 13, 897.
22. Y. Shao, Z. Xiao, C. Bi, Y. Yuan, J. Huang, *Nature Commun*. **2014**, 5, 5784